

# Thick shells in Majumdar-Papapetrou general relativity

**Antares Kleber**

Observatório Nacional - MCT,  
Rua General José Cristino 77, 20921-400, Rio de Janeiro, Brazil, anta@on.br

**José P. S. Lemos**

Centro Multidisciplinar de Astrofísica - CENTRA,  
Departamento de Física, Instituto Superior Técnico, Av. Rovisco Pais 1, 1049-001  
Lisboa, Portugal, lemos@fisica.ist.utl.pt

**Vilson T. Zanchin**

Departamento de Física, Universidade Federal de Santa Maria,  
97119-900 Santa Maria, RS, Brazil zanchin@ccne.ufsm.br

## Abstract.

The Majumdar-Papapetrou system is the subset of the Einstein-Maxwell-charged dust matter theory, when the charge of each particle is equal to its mass. Solutions for this system are less difficult to find, in general one does not need even to impose any spatial symmetry a priori. For instance, any number of extreme Reissner-Nordström solutions (which in vacuum reduce to extreme Reissner-Nordström black holes) located at will is a solution. In matter one can also find solutions with some ease. Here we find an exact solution of the Majumdar-Papapetrou system, a spherically symmetric charged thick shell, with mass  $m$ , outer radius  $r_o$ , and inner radius  $r_i$ . This solution consists of three regions, an inner Minkowski region, a middle region with extreme charged dust matter, and an outer Reissner-Nordström region. The matching of the regions, obeying the usual junction conditions for boundary surfaces, is continuous. For vanishing inner radius, one obtains a Bonnor star, whereas for vanishing thickness, one obtains an infinitesimally thin shell. For sufficiently high mass of the thick shell or sufficiently small outer radius, it forms an extreme Reissner-Nordström quasi-black hole, i.e., a star whose gravitational properties are virtually indistinguishable from a true extreme black hole. This quasi-black hole has no hair and has a naked horizon, meaning that the Riemann tensor at the horizon on an infalling probe diverges. At the critical value, when the mass is equal to the outer radius,  $m = r_o$ , there is no smooth manifold. Above the critical value when  $m > r_o$  one has an extreme black hole with matter inside and no singularities, signaling a change of topology. These systems are neutrally stable. Many of these properties are similar to the properties found for gravitational monopoles.

## 1. Introduction

One can couple Newtonian gravitation to Coulomb electric fields without much effort. A particle with mass  $m_1$  and charge  $q_1$  is certainly a solution of the system. If  $q_1 = m_1$ , then one can put a second particle with  $q_2 = m_2$ , and  $q_1$  and  $q_2$  having the same sign, anywhere. This is also a solution since the Coulomb repulsion compensates exactly for Newtonian attractive force. And of course, one can then put any number of particles, such that for each one the mass equals the charge and the charges have all the same sign. One can go further, distribute the particles continuously to make a fluid, such that the energy density  $\rho$  and the charge density  $\rho_e$  of the charged fluid obey  $\rho_e = \rho$ , and find this is going to be a solution of the Newtonian-Coulomb gravitation. There are other solutions for the Newtonian-Coulomb gravitation, which do not have  $\rho_e = \rho$ , but in these cases the density profile is singular somewhere, or one has to add some pressure to the fluid.

The general relativistic version of the Newtonian-Coulomb gravitation is the Einstein-Maxwell system which admits a vacuum spherically symmetric, particle like solution, given by the Reissner-Nordström metric [1, 2]. For pure vacuum this solution represents a charged black hole when the mass is greater than the charge, an extreme charged black hole when the mass is equal to the charge, and a naked singularity when the mass is smaller than the charge. Weyl in 1917 also had the idea of studying vacuum general relativity and electromagnetism together [3]. Upon further imposing axial symmetry he showed that if there is a functional relationship between the  $g_{tt}$  metric component and the electric potential  $\varphi$ , that relation should be of the form  $g_{tt} = 1 + B\varphi + \varphi^2$ . In 1947 Majumdar [4] showed further that this relation holds for no spatial symmetry at all, axial symmetry being a particular case. Moreover, he showed that if  $g_{tt} = (1 + C\varphi)^2$ , i.e., the above relation is a perfect square, then the spatial metric is conformal to the flat metric, the equations of the system reduce to a master equation of the Poisson type, and the system needs not to be a vacuum system, one can have charge matter with the charge density  $\rho_e$  equal to the energy density  $\rho$ ,  $\rho_e = \rho$ , thus finding the general relativity counterparts to the Newtonian-Coulomb gravitational solutions. Papapetrou explored the same set of ideas, his paper was submitted one month before that of Majumdar [5]. In vacuum,  $\rho_e = \rho = 0$ , the Poisson type equation reduces to the Laplace equation, and any number of extreme Reissner-Nordström black holes located at will is a solution, as was elucidated by Hartle and Hawking [6]. For non vacuum systems, systems with  $\rho_e = \rho$ , the Poisson equation to be solved is more complicated and one usually imposes additional symmetries. Along this line, new solutions were found and discussed by Das [7] and several other authors [8]-[18]. Bonnor and collaborators, in a series of papers, have further developed the field, by constructing spherical symmetric Majumdar-Papapetrou charged stars [19]-[23], as well as stars of other shapes, ellipsoidal for instance [24]. Further developments appeared in Lemos and Weinberg [25] where the causal structure and physical properties of new Majumdar-Papapetrou stars were analyzed. All these solutions may have some

astrophysical appeal, since extreme dust matter can be realized in nature with slightly ionized dust (for instance, a dust particle with  $10^{18}$  neutrons and 1 proton, or an equivalent configuration, realizes extreme dust matter). The equilibrium needed for the dust to be ionized, such that  $\rho_e = \rho$  always, is certainly precarious but possible. Note further that the Majumdar-Papapetrou solutions, both in vacuum and in matter, are also of great importance in supergravity and superstring theories since, when embedded in these extended gravities, they are supersymmetric [26, 27], and saturate a bound on the charge, the charge is equal to the mass, being then called BPS (Bogomolnyi-Prasad-Sommerfield) objects. For instance, low-energy superstring theory admits a series of Majumdar-Papapetrou BPS type solutions in higher dimensions, extreme black extended objects, which can be constructed from extreme black holes by arraying in specific directions (see, e.g. [28]), a process similar to finding charged dust solutions.

Drawing on the work of Bonnor and collaborators [20]-[22] and on the techniques developed in [25], we report here on a new spherical symmetric Majumdar-Papapetrou star, a thick shell, made of three regions: an interior flat part described by the Minkowski metric up to radius  $r_i$ , a middle matter part, from  $r_i$  to  $r_o$ , described by extreme matter  $\rho = \rho_e$  with an appropriate metric, and an exterior region, from  $r_o$  to infinity, described by the extreme Reissner-Nordström solution. The appearance of the three regions is novel. In section II we present the Majumdar-Papapetrou system in harmonic coordinates, which are the ones appropriate to find the solution. In section III we present the solution in Schwarzschild coordinates which are the good ones to study the properties of the system. In section IV we conclude.

## 2. The thick shell solution in harmonic coordinates: Equations and solution

### 2.1. Equations

We will study Einstein-Maxwell theory coupled to charged dust (charged matter with zero pressure). The equation for the Einstein-Maxwell-charged dust system is given by ( $G = c = 1$ )

$$G_{ab} = 8\pi \left( T_{ab}^{\text{dust}} + T_{ab}^{\text{em}} \right), \quad (1)$$

where  $G_{ab}$  is the Einstein tensor.  $T_{ab}^{\text{dust}}$  is the dust part of the stress-energy tensor

$$T_{ab}^{\text{dust}} = \rho u_a u_b, \quad (2)$$

with  $\rho$  being the energy-density, and  $u_a$  is the four-velocity of the fluid.  $T_{ab}^{\text{em}}$  is the electromagnetic part of the stress-energy tensor

$$T_{ab}^{\text{matter}} = \frac{1}{4\pi} \left( F_a^c F_{bc} - \frac{1}{4} g_{ab} F^{cd} F_{cd} \right), \quad (3)$$

with  $F_{ab}$  being the Maxwell tensor. The two Maxwell equations, are

$$F_{a;b}^b = 4\pi j_a, \quad (4)$$

$$F_{[ab;c]} = 0. \quad (5)$$

where  $j_a = \rho_e u_a$  is the electric four-current,  $\rho_e$  is the electric charge density of the dust, and  $[\ ]$  denotes anti-symmetrization. Equation (5) permits to define a vector potential  $A_a$  such that

$$F_{ab} = A_{b,a} - A_{a,b}. \quad (6)$$

Now, for a static pure electric system one can make the choice

$$u_a = \frac{\delta_a^0}{U}, \quad A_a = \delta_a^0 \varphi, \quad (7)$$

where  $U$  and  $\varphi$  are functions of the spatial coordinates,  $U$  being identified with the gravitational potential, and  $\varphi$  with the electric potential. Furthermore, it was then shown by Majumdar [4] in a very elegant paper, that in the special case of extreme dust matter, i.e., when the energy density is equal to the charge density,

$$\rho_e = \rho, \quad (8)$$

the metric can be put in form

$$ds^2 = -\frac{dt^2}{U^2} + U^2 (dx^2 + dy^2 + dz^2), \quad (9)$$

where  $(t, x, y, z)$  are called harmonic coordinates. The Einstein-Maxwell-extreme dust matter system (1) then can be reduced to the following system of equations,

$$\nabla^2 U = -4\pi \rho U^3, \quad (10)$$

$$\varphi = 1 - \frac{1}{U}, \quad (11)$$

with  $\nabla^2 \equiv \frac{\partial^2}{\partial x^2} + \frac{\partial^2}{\partial y^2} + \frac{\partial^2}{\partial z^2}$  is the flat Laplacian operator. We should comment that there is a possible choice for the sign of the charge density, strictly speaking  $\rho_e = \pm \rho$ . Above we have chosen the plus sign, had we chose the minus sign the sign of the electric potential also changes, i.e.,  $\varphi = 1 + 1/U$ . In order to not carry a  $\pm$  label we stick to the plus sign of the charge density, knowing the results will not be altered.

Thus, from equation (10) one sees that solutions with no spatial symmetry at all, are solutions of this system. This is because particles with charge equal to mass, or matter systems with  $\rho_e = \rho$ , exert zero force upon each other, or within themselves, a result valid in both Newtonian gravitation and general relativity, so that they can be distributed at will. Solutions of this Einstein-Maxwell-extreme dust matter system are generically called Majumdar-Papapetrou solutions [4, 5], a particular instance of these are the Bonnor stars [19]-[24].

## 2.2. Thick shell solution with three regions: interior flat, middle charged dust, exterior extreme Reissner-Nordström

Here we want to find a spherical symmetric solution in which case the line element (9) should be written as

$$ds^2 = -\frac{dt^2}{U^2} + U^2 [dR^2 + R^2 (d\theta^2 + \sin^2 \theta d\phi^2)], \quad (12)$$

where  $U = U(R)$ , and the three-dimensional Laplacian is now  $\nabla^2 U = \frac{1}{R^2} \frac{\partial}{\partial R} \left( R^2 \frac{\partial U}{\partial R} \right)$ . The field equation (10) can be solved by guessing a potential  $U$ , and then finding  $\rho$ . The solution is then complete because  $\rho_e$  and  $\varphi$  follow directly. If the solution is physically acceptable, then it is of interest. One such spherical symmetric solution has been found by Bonnor and Wickramasuriya [20]-[22], describing a matter configuration from  $R = 0$  to  $R = R_o$ , and then vacuum outside, given by the extreme Reissner-Nordström metric. We find here a non trivial extension of this Bonnor star solution by adding a region internal to the matter that is flat, described by the Minkowski metric. We display for the first time a global Majumdar-Papapetrou exact solution that is composed of three regions, the interior vacuum Minkowski, the middle matter region, and the exterior extreme Reissner-Nordström electrovacuum region.

The system is characterized by its ADM mass  $m$ , and its inner and outer harmonic radii  $R_i$  and  $R_o$ , respectively. The solution for  $U(r)$  (and thus for the system) is

$$U_{\text{flat}} = 1 + \frac{m}{R_o} \left( 1 + \frac{R_o - R_i}{2R_o} \right), \quad 0 \leq R \leq R_i, \quad (13)$$

$$U_{\text{matter}} = 1 + \frac{m}{R_o} \left[ 1 + \frac{(R_o - R_i)^2 - (R - R_i)^2}{2R_o(R_o - R_i)} \right], \quad R_i \leq R \leq R_o, \quad (14)$$

$$U_{\text{RN}} = 1 + \frac{m}{R}, \quad R_o \leq R. \quad (15)$$

With  $U$  we can find through Equation (12) the metric for the whole spacetime, and through Equation (11) the electric potential  $\varphi$ . The energy density is zero outside matter, and in the matter it is found using Equation (10),  $\rho = \frac{3m}{4\pi R_o^3} \frac{R_o}{R_o - R_i} \frac{1 - \frac{2}{3} \frac{R_i}{R}}{U_{\text{matter}}^3}$ , with the charge density being then  $\rho_e = \rho$ . Regular boundary conditions at the center and at infinity are obeyed, at the center the metric and matter fields are regular, and at infinity spacetime is asymptotically flat, the electric field decays as a Coulomb field, and the extreme dust matter density is zero. Moreover, since there are two interfaces one has to check whether the junction conditions are obeyed at these boundaries. Indeed, it is found that they are obeyed, with no need for thin shells, see Section 3.2 and the Appendix B for more details. If one puts  $R_i = 0$  one gets the Bonnor solution [21] with two regions, the matter region and the exterior extreme Reissner-Nordström region. Note also that on using (13) on (12) one clearly gets the Minkowski metric, but not in the usual form. To do so one has to define a  $\bar{t}$  such that  $\bar{t} = t/U_{\text{flat}}$ , and an  $\bar{R}$  such that  $\bar{R} = U_{\text{flat}} R$ . The coordinates in the matter and electrovacuum regions would change accordingly. We will not do it here, since it is not necessary and gets cumbersome.

The use of harmonic coordinates is good for finding solutions, as Majumdar has shown [4], but the interpretation of the solution is best done in Schwarzschild coordinates, where the radial coordinate  $r$  yields a measure of circumferences, or of areas, of the type we are used to in flat space.

### 3. The thick shell solution in Schwarzschild coordinates: Physical features

#### 3.1. Equations

In Schwarzschild coordinates we write the metric in the form

$$ds^2 = -B(r) dt^2 + A(r) dr^2 + r^2 (d\theta^2 + \sin^2 \theta d\phi^2), \quad (16)$$

and the electric Maxwell field is written as

$$A_0 = \varphi(r), \quad A_i = 0. \quad (17)$$

One can use Equations (1)-(6) to find three non-trivial equations,

$$\frac{(AB)'}{AB} = 8\pi r \rho A, \quad (18)$$

$$\left[ r \left( 1 - \frac{1}{A} \right) \right]' = 8\pi r^2 \rho + \frac{r^2}{AB} \varphi'^2, \quad (19)$$

$$\frac{1}{r^2 \sqrt{A}} \left[ \frac{r^2}{\sqrt{AB}} \varphi' \right]' = -4\pi \rho_e. \quad (20)$$

Upon using the Majumdar-Papapetrou condition  $\rho_e = \rho$  one should be able to find the thick shell solution in Schwarzschild coordinates. Of course, it is much easier to make a simple coordinate transformation from the solution in harmonic spherical coordinates  $(t, R, \theta, \phi)$  to the solution in Schwarzschild coordinates  $(t, r, \theta, \phi)$ . This we will do next.

#### 3.2. The thick shell solution

Schwarzschild coordinates are good for interpreting the solution. In these coordinates the metric takes the form (16). One sees that the coordinate  $r$  has some physical meaning, the area of a sphere of constant  $r$  is given by  $4\pi r^2$ . By inspection of Equations (12) and (16) one finds that the relation between  $r$  and  $R$  is

$$r = U R. \quad (21)$$

Then, one gets  $B(r) = 1/U^2$ . From (21) one finds  $dr/[1 + \frac{R}{U} \frac{dU}{dR}(r)] = U dR$ . Thus  $A(r) = 1/[1 + \frac{R}{U} \frac{dU}{dR}(r)]^2$ . Note that from (21) one gets  $R$  as a function of  $r$ , in general implicitly, but in some cases, such as here, it can be solved explicitly. Now we have to transform coordinates in each region. We begin with the easiest ones, the exterior and interior vacua regions, and then do the matter region. The three regions are schematically represented in Figure 1.

The exterior Reissner-Nordström region is trivial, and we will do it first. From Equations (15) and (21) one gets, for the whole Reissner-Nordström region

$$R = r - m, \quad (22)$$

and in particular at the boundary, one has

$$R_o = r_o - m. \quad (23)$$

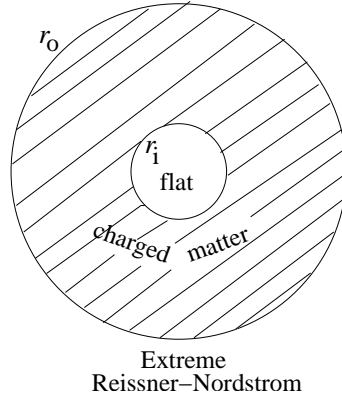


Figure 1 - A schematic drawing of the three regions of the thick shell solution: the interior flat region, the middle charged matter region, and the exterior extreme Reissner-Nordström region.

For the interior flat region one finds from Equations (13) and (21) that  $R_i$  is a function of  $r_i$  and  $r_o$ , i.e.,  $R_i = R_i(r_i, r_o)$ , and we define  $f_i \equiv R_i(r_i, r_o)$ . Then

$$f_i = \left[ \frac{r_o}{m} + \frac{1}{2} - \sqrt{\left( \frac{r_o}{m} + \frac{1}{2} \right)^2 - \frac{2r_i}{m}} \right] \left( \frac{r_o}{m} - 1 \right) m. \quad (24)$$

Then again from Equations (13) and (21) one has for the whole flat region

$$R = \frac{r}{1 + \frac{m}{r_o - m} \left[ 1 + \frac{r_o - m - f_i}{2(r_o - m)} \right]}. \quad (25)$$

For the matter region, from Equations (14) and (21), one has to solve a nasty cubic equation for  $R$ , giving  $R$  as a function of  $r$ . We denote this function by  $f(r)$ , i.e., in the matter region,

$$R = f(r), \quad (26)$$

and give  $f(r)$  in the Appendix A. Note that  $f(r_i) = f_i$ .

We can now write the metric in Schwarzschild coordinates for  $0 \leq r < \infty$ . For the interior flat region is,

$$ds^2 = - \left( \frac{f_i}{r_i} \right)^2 dt^2 + dr^2 + r^2 (d\theta^2 + \sin^2 \theta d\phi^2), \quad 0 \leq r \leq r_i. \quad (27)$$

For the matter region is

$$ds^2 = - \left( \frac{f(r)}{r} \right)^2 dt^2 + \frac{dr^2}{\left( 1 - \frac{f^2(r)}{r} \frac{m[f(r) - f_i]}{(r_o - m)^2 (r_o - m - f_i)} \right)^2} + r^2 (d\theta^2 + \sin^2 \theta d\phi^2), \quad r_i \leq r \leq r_o. \quad (28)$$

For the exterior Reissner-Nordström region one has

$$ds^2 = - \left( 1 - \frac{m}{r} \right)^2 dt^2 + \frac{dr^2}{\left( 1 - \frac{m}{r} \right)^2} + r^2 (d\theta^2 + \sin^2 \theta d\phi^2), \quad r_o \leq r. \quad (29)$$

The three regions join continuously, since the metric and the extrinsic curvature of the two boundaries match, as we show in Appendix B. A quick way to see this is to note that at the inner boundary the  $g_{tt}$  part obviously matches, and the  $g_{rr}$  part also matches since in the matter region one has  $g_{rr} = 1$  at  $r = r_i$ . In the outer boundary one has  $f(r_o)/r_o = 1 - m/r_o$ , so the  $g_{tt}$  terms match, and as well the  $g_{rr}$  are identical at  $r_o$ . One can also check that  $\frac{\partial f(r)/r}{\partial r}\bigg|_{r_i} = 0$  so that the first derivatives of  $g_{tt}$  match at the inner boundary. As well,  $\frac{\partial f(r)/r}{\partial r}\bigg|_{r_o} = 2\left(1 - \frac{m}{r_o}\right)\frac{m}{r_o^2}$ , so that the first derivatives of  $g_{tt}$  match at the outer boundary. The derivatives of  $g_{rr}$  do not match, but that is expected for a boundary surface. So  $g_{rr}$  is  $C^0$  at both boundaries and the other metric functions are  $C^1$  or higher. This means that the Israel junction conditions are satisfied, yielding a boundary surface (see also Appendix B). With some extra effort one can smooth out the  $g_{rr}$  component at the boundaries, so that  $g_{rr}$  is  $C^1$  or  $C^2$ , but we will not do it here.

The electric potential is taken from Equation (11),  $\varphi = 1 - \frac{1}{U}$ , but now  $U$  is seen as a function of  $r$ , (alternatively,  $\varphi$  can be taken from  $\varphi = 1 - \sqrt{|g_{tt}|}$  with the  $|g_{tt}|$  for the three regions given in Equations (27)-(29)). Thus, we have

$$\varphi = 1 - \frac{1}{1 + \frac{m}{r_o - m} \left(1 + \frac{r_o - m - f_i}{2(r_o - m)}\right)}, \quad 0 \leq r \leq r_i, \quad (30)$$

$$\varphi = 1 - \frac{1}{U_{\text{matter}}}, \quad r_i \leq r \leq r_o, \quad (31)$$

$$\varphi = 1 - \left(1 - \frac{m}{r}\right) = \frac{m}{r}, \quad r_o \leq r, \quad (32)$$

where in Equation (31),  $U_{\text{matter}}(r)$  is now

$$U_{\text{matter}} = 1 + \frac{m}{(r_o - m)} \left[1 + \frac{(r_o - m - f_i)^2 - (f(r) - f_i)^2}{2(r_o - m)(r_o - m - f_i)}\right], \quad r_i \leq r \leq r_o, \quad (33)$$

The electric potential is continuous and smooth at the boundaries.

The energy density can be also calculated in these coordinates. We have

$$\rho = 0, \quad 0 \leq r < r_i, \quad (34)$$

$$\rho = \frac{3m}{4\pi(r_o - m)^2 (r_o - m - f_i)} \frac{1 - \frac{2f_i}{3f(r)}}{U_{\text{matter}}(r)^3}, \quad r_i \leq r \leq r_o, \quad (35)$$

$$\rho = 0, \quad r_o < r, \quad (36)$$

where  $U_{\text{matter}}(r)$  is given in (33). The energy density is a step function at  $r_i$  and  $r_o$ , but this is no problem, jumps in the energy density are allowed. It is easy to check that the energy density  $\rho$  is everywhere positive in the thick shell, as it should for a realistic fluid description. The charge density follows from  $\rho_e = \rho$ .

Again, regular boundary conditions at the center and at infinity are obeyed, at the center the metric and matter fields are regular, and at infinity spacetime is asymptotically flat, the electric field decays as a Coulomb field, and the extreme dust matter density is zero. Moreover, as we have just showed the junction conditions at the outer and inner boundaries are also obeyed.

### 3.3. Physical properties of the thick shell

3.3.1. *From low gravitation configurations to extreme quasi-black holes* The thick shell solution is given by the equations of the last subsection (27)-(36). The solutions are characterized by the mass  $m$ , the outer and the internal radius,  $r_o$  and  $r_i$ . An important dimensionless quantity is the ratio of the mass to outer radius,

$$a = \frac{m}{r_o}. \quad (37)$$

This quantity is a measure of how general relativistic is the system. Small  $a$  means the thick shell is very dispersed, Newtonian gravitation might suffice. For large  $a$  general relativistic effects come into play and eventually at  $a_{\text{crit}} \rightarrow 1$  ( $m \rightarrow r_o$ ) an event horizon is about to form. This is displayed in Figure 2, where we draw the dependence of the metric, electric and density potentials as a function of radius, for  $a$  small and  $a_{\text{crit}}$ .

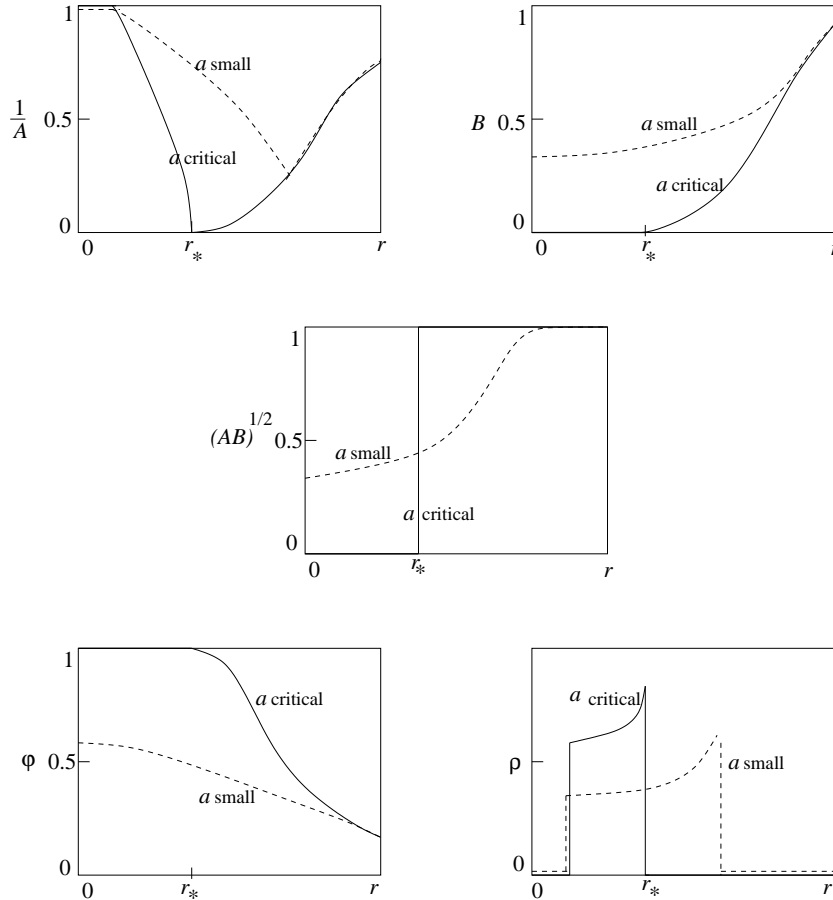


Figure 2 - Behaviour of the metric, electric and matter functions in terms of the radius  $r$ . Note that  $r_*$  is  $r_o$  critical.

The function  $A$  signals the appearance of an event horizon, when  $1/A$  passes through a zero, a horizon is formed, in this case it should be an extreme horizon, since  $1/A$  gets a double zero (it is not strictly a double zero, since it is not smooth at  $r_o$ , but with some care, either analytically or numerically one can smooth it out). The function  $B$  is the redshift function, with  $B = 0$  meaning infinite redshift. It is seen from equation

(24) that for  $a_{\text{crit}}$  the parameter  $f_i$  is identically zero, which means  $B = 0$  in the region  $0 \leq r \leq r_i$ . This is true also in the region  $r_i < r \leq r_o$ , as can be checked from equations (A.5) and (A.6) for the function  $f(r)$  in the Appendix A. Hence, at  $a_{\text{crit}}$  the redshift is infinite at the horizon and in the whole region inside. This means that in fact a true black hole does not form, since inside there is no smooth manifold. One says that, at  $a_{\text{crit}} \rightarrow 1$ , a quasi-horizon forms and the object is a quasi-black hole [25]. The product  $(AB)^{1/2}$  is an important function, it gives whether the horizon is naked or not, see the last two paragraphs of this section for a more specific discussion on this point. The electric potential  $\varphi$  shows that at  $a_{\text{crit}}$ , the electric potential outside the horizon is Coulombian, the black hole has no hair. The density field, shows a very interesting feature, when the star is about to form a quasi-black hole, there is still equilibrium, nothing special happens, its surface being a quasi-horizon with radius  $r_*$  arbitrarily closed to the extreme Reissner-Nordström black hole radius  $r_h$ . Note that the figures displayed in Figure 2 correspond to Figures 2-6 of [25]. The curves for  $A$ ,  $B$ ,  $(AB)^{1/2}$  and  $\phi$  show similar behaviors in both cases, since for  $r > r_o$  they are the same functions and for  $r < r_o$  they are power law functions.

There are two points worth noting in the meantime: (i) It is interesting that on one hand these thick shell Majumdar-Papapetrou stars superseed the Buchdall bounds for perfect fluid matter stars [29], where the radius of the star obeys  $r_{\text{star}} \geq \frac{9}{8}r_h$ , with  $r_h = 2m$ , on the other hand, when they are about to form a black hole the spacetime turns into a degenerate one, so that there is no smooth manifold. (ii) Although we do not discuss in detail in this paper what happens above criticality, i.e., for  $a > a_{\text{crit}}$  ( $m > r_o$ ), we note that in this case one has a shell of matter inside an extreme black hole at  $r_h = m$ . In addition such a solution is everywhere free from curvature singularities. Following a theorem by Borde [30] this means that the topology of spacelike slices in this black hole spacetime changes from a region where they are noncompact to a region where they are compact, in the interior. An example of this behavior appears in the Bardeen model [31, 32].

We now dwell further on the nakedness of the extreme horizon formed. A horizon is naked when the tidal forces suffered by an infalling particle at the horizon are infinite [33]. The important function here is the product  $(AB)^{1/2}$ , because it gives whether the horizon is naked or not. Schwarzschild and Reissner-Nordström horizons are not naked, nothing special happens to a particle passing through their horizons. However, here these tidal forces tend to infinite. To see this, send a massive particle from a large radius  $r$ , through the thick shell, so that it turns around and comes back [34]. Due to the staticity and spherical symmetry of the metric one can define a conserved energy and a conserved angular momentum per unit mass for the particle,  $J = r^2 \frac{d\phi}{d\tau}$ ,  $E = B(r) \frac{dt}{d\tau}$ . Then from Equation (16) one has

$$\frac{d\tau}{dr} = \frac{(AB)^{1/2}}{\left[ E^2 - B \left( \frac{J^2}{r^2} + 1 \right) \right]^{1/2}}. \quad (38)$$

We are interested in the quasi-horizon configuration, the one which is about to form a horizon but not quite. Call the radius of this configuration  $r_*$ . Call also  $\frac{1}{A}|_{r_*} = \epsilon$  where  $\epsilon \rightarrow 0$  at the critical solution. Then one has from Equation (38) that the particle spends a proper time inside the star of the order of  $\Delta\tau \simeq \frac{r_*}{E}(AB)^{1/2}|_{r_*} \sim \epsilon^{1/2}$  (indeed, for  $1 - \frac{r}{m} = \epsilon$  and  $\frac{r_o}{m} - 1 = \alpha\epsilon$ , with  $\alpha$  a number of order one or so and  $\epsilon \ll 1$ , one has  $f(r) = (r_o - m)(1 - \sqrt{\frac{2}{3}\epsilon})$ , and thus  $1/\sqrt{A} = 1 - (m/r)[f(r)^3/(r_o - m)^3] = 3\sqrt{\frac{2}{3}\epsilon}$ , so  $1/A = 6\epsilon$ , and  $\sqrt{B} = f(r)/r = \alpha\epsilon$ , so that  $(AB)^{1/2} = \alpha\epsilon^{1/2}$ ). For the quasi-horizon this time is extremely short, and at the critical configuration is zero, since  $(AB)^{1/2}$  vanishes for  $r < r_*$ . It was shown in [34] that for this type of configurations the local Riemann tensor at the horizon, i.e., the Riemann tensor as measured by a freely falling observer passing through the horizon, is proportional to the inverse of the square of the proper time a particle takes inside the quasi-horizon, i.e.,  $R_{\text{iemann}} \sim \frac{1}{(\Delta\tau)^2}$ . Since  $\Delta\tau$  goes to zero, the local Riemann tensor diverges, and the horizon is naked.

Another interesting time, is the time  $\Delta t$  the particle takes in its trip for a coordinate observer. One can show that this time is  $\Delta t \sim \frac{r_*}{\epsilon}$ . At the quasi-critical solution this time is arbitrarily large. Thus, for an external observer the particle takes an arbitrarily quasi infinite time to come back. The observer cannot probe the inside, and associates it with an entropy for the star (see [34] for a discussion on quasi-black hole entropy).

*3.3.2. Penrose diagrams* One can draw the Penrose diagrams for two configurations, for the quasi-black hole with  $a \rightarrow m/r_o$  quasi-critical, and for the black hole with the same mass parameter, see Figure 3. For the quasi-black hole, the Penrose diagram is the same as for  $a$  small. In these cases, the spacetime is asymptotically Minkowskian, and the origin of the coordinates  $r = 0$  and the surface of the thick shell star  $r_o = r_*$  are timelike surfaces. On the other hand, for the true black hole, spacetime is still asymptotically Minkowskian, with  $r_h$  being a true horizon, whereas  $r = 0$  is now a curvature singularity.

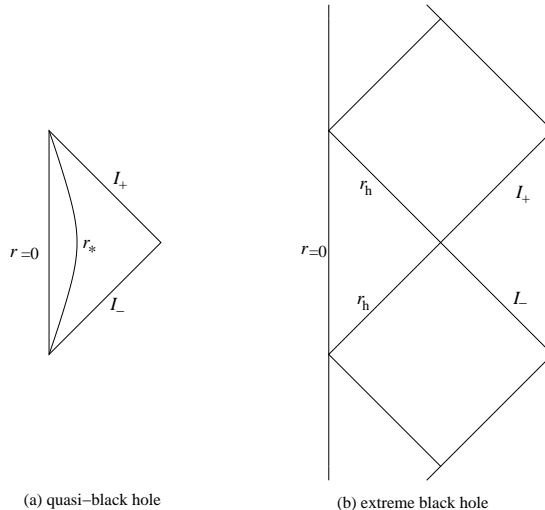


Figure 3 - Penrose diagrams for (a) the quasi-black hole, and (b) the extreme black hole, are shown.

Note that at criticality, ( $m = r_o$ ), there is no Penrose diagram for the quasi-black hole since time has disappeared from spacetime, the solution is now degenerate. Above criticality, ( $m > r_o$ ), one would have to draw a Penrose diagram along the lines suggested by Borde [30], where the interior is free of singularities. It would be interesting to find some possible non singular continuation from sub-critical to supercritical solutions.

### 3.4. Two limits: stars and thin shells

There are two interesting limits of the Majumdar-Papapetrou thick shell solution.

*3.4.1. Bonnor stars* If one takes the limit of a vanishing inner radius  $r_i = 0$  one obtains a Bonnor star [20]-[22]. This solution has two regions, the interior from  $r = 0$  to  $r = r_o$ , made of extreme charged matter, and the exterior, an extreme Reissner-Nordström region. The Bonnor star has the same properties of the thick shell solution, when the star is compact enough it forms an extreme Reissner-Nordström quasi-black hole with a naked horizon (see [25] for more details).

*3.4.2. Infinitesimally thin shells* Another important limit is the infinitesimally thin shell limit, when the thickness of the shell goes to zero,  $r_i \rightarrow r_o$ . The important quantity to keep track is the energy density  $\rho$  (an energy per unit volume) that must go over into a surface energy density  $\sigma$  (an energy per unit area). From Equation (35) one obtains, when  $r_o \rightarrow r_i$ ,  $\rho = \frac{m}{4\pi r_o^2} \left( \frac{1 - \frac{m}{r_o}}{r_o - r_i} \right)$ , in first order in  $r_o - r_i$ . The proper surface energy density of the thin shell should be defined as  $\sigma = \lim_{r_o \rightarrow r_i} \left( \frac{r_o - r_i}{1 - \frac{m}{r_o}} \right) \rho$ , where the factor  $(r_o - r_i)$  is as in Newtonian theory, and the factor  $1/(1 - \frac{m}{r_o})$  takes care of the proper length (see metric (16)). Thus, we find

$$\sigma = \frac{m}{4\pi r_o^2}, \quad (39)$$

as it is expected for an infinitesimally thin shell. The three regions are now, an inner flat region, a thin shell, and an exterior Reissner-Nordström vacuum. The metric is now

$$ds^2 = - \left( 1 - \frac{m}{r_o} \right)^2 dt^2 + dr^2 + r^2 (d\theta^2 + \sin^2 \theta d\phi^2), \quad 0 \leq r < r_o, \quad (40)$$

$$ds^2 = - \left( 1 - \frac{m}{r_o} \right)^2 dt^2 + r^2 (d\theta^2 + \sin^2 \theta d\phi^2), \quad r = r_o, \quad (41)$$

$$ds^2 = - \left( 1 - \frac{m}{r} \right)^2 dt^2 + \frac{dr^2}{\left( 1 - \frac{m}{r} \right)^2} + r^2 (d\theta^2 + \sin^2 \theta d\phi^2), \quad r_o \leq r. \quad (42)$$

Note that the  $g_{rr}$  component has a step at  $r_o$  from 1 to  $1/\left( 1 - \frac{m}{r_o} \right)^2$ , meaning that the junction conditions are not satisfied there. This is a minor problem, one can always see it as a very thin shell (not infinitesimally thin), where there is no discontinuity, although the slope of the  $g_{rr}$  function is very high. The electromagnetic field can be taken from

$\varphi = 1 - \sqrt{|g_{tt}|}$  in equations (40)-(42). The thin shell has analogous properties to the thick shell solution. When it is compact enough, for  $a \rightarrow a_{\text{crit}}$  (i.e.,  $m \rightarrow r_o$ ) it forms an extreme Reissner-Nordström quasi-black hole with a naked horizon. When the precise equality holds,  $a = a_{\text{crit}}$ , the redshift function  $B$  is infinite not only at the horizon but also in the whole region inside, meaning that in fact a true black hole does not form, since inside there is no smooth manifold. This signals a change in topology. Indeed, one can ask what happens for  $a > a_{\text{crit}}$ ,  $m > r_o$ ? From equations (39)-(42) the solution still holds. But now one has a shell of matter at  $r_o$  inside an extreme black hole at  $r_h = m$ . In addition the solution is everywhere free from curvature singularities. Thus it seems that the theorems of Borde [30] apply here, and that in this regime the solutions have a behaviour analogous to the Bardeen model [31, 32]. Note also that for the same mass parameter  $m$  there is also the branch of pure extreme Reissner-Nordström black holes.

#### 4. Conclusions

We have found an exact solution of the Majumdar-Papapetrou system, the thick shell star solution, consisting of three regions, an inner Minkowski region, a middle region with extreme charged matter, and an outer Reissner-Nordström region. The system is neutrally stable, as all the systems of Majumdar-Papapetrou type are. For sufficiently high mass, or sufficiently small outer radius, at almost the critical value, the thick shell forms an extreme Reissner-Nordström quasi-black hole, with no hair and with a naked horizon, i.e., the Riemann tensor at the horizon on an infalling probe diverges. At the critical value there is no smooth manifold. Above the critical value when  $m > r_o$  one has an extreme black hole with matter inside and no singularities, signaling a change of topology. All these properties are similar to the properties found for gravitational monopoles when gravity takes care of the system [34]. In another work we will explore these similarities which are much too striking to pass without some attention [25, 35].

**Acknowledgments:** We thank Erick Weinberg for conversations. JPSL thanks Columbia University for hospitality, and acknowledges financial support from the Portuguese Science Foundation FCT and FSE for support, through POCTI along the III Quadro Comunitario de Apoio, reference number 327/2002. VTZ thanks Observatório Nacional do Rio de Janeiro for hospitality.

## Appendix A. The harmonic coordinate $R$ as a function of the Schwarzschild coordinate $r$ in the matter region

We want to invert the equation

$$r = R U_{\text{matter}} = R \left[ 1 + \frac{m}{R_o} \left( 1 + \frac{(R_o - R_i)^2 - (R - R_i)^2}{2R_o(R_o - R_i)} \right) \right]. \quad (\text{A.1})$$

In order to condense expressions, define

$$a = -\frac{E}{F} - \frac{1}{3} R_i^2, \quad b = \frac{r}{F} + \left( -\frac{2E}{3F} + \frac{2R_i^2}{27} \right) R_i, \quad (\text{A.2})$$

with

$$E = 1 + \frac{m}{R_o} \left( 1 + \frac{R_o - R_i}{2R_o} \right), \quad F = \frac{m}{2R_o^2(R_o - R_i)}, \quad (\text{A.3})$$

where  $R_o = r_o - m$  as in (23), and  $R_i = R_i(r_i, r_o)$  as in (24). Then through further definitions

$$A = {}^3\sqrt{-\frac{b}{2} + \sqrt{\frac{b^2}{4} + \frac{a^3}{27}}}, \quad B = {}^3\sqrt{-\frac{b}{2} - \sqrt{\frac{b^2}{4} + \frac{a^3}{27}}}, \quad (\text{A.4})$$

The solution is  $R = f(r)$ , with

$$f(r) = \frac{2}{3} f_i - \frac{A+B}{2} - \frac{A-B}{2} \sqrt{-3}. \quad (\text{A.5})$$

For  $r$  and  $r_i$  small one finds

$$f(r) - f_i = \frac{2(r_o - m)}{2r_o + m} (r - r_i), \quad (\text{A.6})$$

where we have used (23) and (24).

## Appendix B. The matching conditions of the the thick shell

We will follow Israel [36] to show that the two boundaries at  $r_o$  and  $r_i$  are boundary surfaces, i.e., do not need extraneous thin shells. We need to show that the metric, or first fundamental form, is continuous at the surface,  $g_{ab}^+ = g_{ab}^-$ , and the extrinsic curvature, or second fundamental form, is also continuous,  $K_{ab}^+ = K_{ab}^-$ . For the extrinsic curvature, we note first that, since the surface we use is spherical the normal  $n_a$  to the surface has only a radial component  $n_r = \sqrt{g_{rr}}$ . Then the extrinsic curvature has the form

$$K_{ij}^\pm = -n_r \Gamma_{\alpha\beta}^{r\pm} \frac{\partial x^\alpha}{\partial \xi^i} \frac{\partial x^\beta}{\partial \xi^j}, \quad (\text{B.1})$$

where  $\xi^i$  are the intrinsic coordinates of the surface. Now we analyze the junction at the outer and inner surfaces.

**Outer boundary,  $r = r_o$ :** For the surface  $r_o$  we adopt the metric

$$ds^2 = - \left(1 - \frac{m}{r_o}\right)^2 d\tau^2 + r^2(d\theta^2 + \sin^2 d\phi^2), \quad (\text{B.2})$$

with the intrinsic coordinates  $\xi^i$  being  $\xi^i = (\tau, \theta, \phi)$ . Then one has  $f(r_o)/r_o = 1 - m/r_o$ , so from Equations (28) and (29) one sees that the  $g_{tt}^+$  and  $g_{tt}^-$  match. The  $g_{rr}^+$  and  $g_{rr}^-$  also match, as well as the terms for the angular part. Now, at  $r_o$  coming for the interior one finds  $K_{\tau\tau}^- = -n_r \Gamma_{tt}^{r-} \frac{dt}{d\tau} \frac{dt}{d\tau}$ . By construction  $\frac{dt}{d\tau} = 1$ . One also has  $n_r = \frac{1}{1 - \frac{f^2}{r} \frac{m(f-f_i)}{(r_o-m)^2(r_o-m-f_i)}} \Big|_{r_o} = \frac{1}{1 - \frac{m}{r_o}}$ . Noting that  $\frac{df}{dr} \Big|_{r_o} = 1$  one finds  $\Gamma_{tt}^{r-} = \frac{m(r_o-m)^3}{r_o^5}$ . Thus,  $K_{\tau\tau}^- = \frac{m(r_o-m)^2}{r_o^4}$ . The extrinsic curvature coming from the exterior Reissner-Nordström region can also be calculated, one finds  $K_{\tau\tau}^+ = \frac{m(r_o-m)^2}{r_o^4}$ . So they match. One can also check that  $K_{\theta\theta}$  and  $K_{\phi\phi}$  also match.

**Inner boundary,  $r = r_i$ :** For the surface  $r_i$  we adopt the metric

$$ds^2 = - \left(\frac{f_i}{r_i}\right)^2 d\tau^2 + r^2(d\theta^2 + \sin^2 d\phi^2), \quad (\text{B.3})$$

From Equations (27) and (28) one sees that the  $g_{tt}$  part matches, and the  $g_{rr}$  part also matches since in the matter region one has  $g_{rr} = 1$  at  $r = r_i$ . Likewise for  $g_{\theta\theta}$  and  $g_{\phi\phi}$ . Now, at  $r_i$  coming for the matter one finds  $K_{\tau\tau}^+ = -n_r \Gamma_{tt}^{r-} \frac{dt}{d\tau} \frac{dt}{d\tau}$ . By construction  $\frac{dt}{d\tau} = 1$ . One also has  $n_r = 1$ . Noting that  $\frac{df}{dr} \Big|_{r_i} = \frac{f}{r}$  one finds  $\Gamma_{tt}^{r-} = 0$ . Thus,  $K_{\tau\tau}^+ = 0$ . The extrinsic curvature coming from the interior flat region can also be calculated, one finds  $K_{\tau\tau}^- = 0$ . So they match. One can also check that  $K_{\theta\theta}$  and  $K_{\phi\phi}$  also match.

So the metric and the extrinsic curvature are continuous as is required. The electric potential  $\varphi$  and its first derivative at the boundaries are continuous as is also required.

## References

- [1] H. Reissner, Ann. Physik **50**, 106 (1916).
- [2] G. Nordström, Proc. Kon. Ned. Akad. Wet. **20**, 1238 (1918).
- [3] H. Weyl, Ann. Physik **54**, 117 (1917).
- [4] S. D. Majumdar, Phys. Rev. **72**, 390 (1947).
- [5] A. Papapetrou, Proc. Roy. Irish Acad. A **51**, 191 (1947).
- [6] J. B. Hartle and S. W. Hawking, Comm. Math. Phys. **26**, 87 (1972).
- [7] A. Das, Proc. R. Soc. London A **267**, 1 (1962).
- [8] J. M. Cohen and M. D. Cohen, Nuovo Cim. **60**, 241 (1969).
- [9] R. Gautreau and R. B. Hoffman, Nuovo Cim. B **16**, 162 (1973).
- [10] A. K. Raychaudhuri, Ann. Inst. Henri Poincaré A **22**, 229 (1975).
- [11] P. S. Florides, Nuovo Cim. A **42**, 343 (1977).
- [12] D. R. Brill, Contribution to Festschrift volume for Engelbert Schucking (1997), gr-qc/9709063.
- [13] M. Gürses, Phys. Rev. D **58**, 044001 (1998).
- [14] D. Lynden-Bell, J. Bicak and J. Katz, Annals Phys. **271**, 1 (1999).
- [15] B. Guilfoyle, Gen. Rel. Grav. **31**, 1645 (1999).
- [16] D. Ida, Prog. Theor. Phys. **103**, 573 (2000).
- [17] V. Varela, Gen. Rel. Grav. **35**, 1815 (2003).

- [18] B. V. Ivanov, Phys. Rev. D. **65** (2002) 104001.
- [19] W. B. Bonnor, Zeitschrift Phys. **160**, 59 (1960).
- [20] W. B. Bonnor and S. B. P. Wickramasuriya, Int. J. Theor. Phys. **5**, 371 (1972).
- [21] W. B. Bonnor and S. B. P. Wickramasuriya, Mon. Not. R. Astr. Soc. **170**, 643 (1975).
- [22] W. B. Bonnor, Class. Quantum Grav. **16**, 4125 (1999).
- [23] W. B. Bonnor, Gen. Rel. Grav. **12**, 453 (1980).
- [24] W. B. Bonnor, Class. Quantum Grav. **15**, 351 (1998).
- [25] J. P. S. Lemos and E. J. Weinberg, Phys. Rev. D **69**, 104004 (2004).
- [26] G. W. Gibbons and C. M. Hull, Phys. Lett. B **109**, 190 (1982).
- [27] K. P. Tod, Phys. Lett. B **121**, 241 (1983).
- [28] A. W. Peet, “TASI lectures on black holes in string theory”, hep-th/0008241 (2000).
- [29] H. A. Buchdall, Austr. J. Phys. **9**, 13 (1956).
- [30] A. Borde, Phys. Rev. D **55**, 7615 (1997).
- [31] E. Ayón-Beato, A. García, Phys. Rev. Lett. **80**, 5056 (1998).
- [32] E. Ayón-Beato, A. García, Phys. Lett. B **493**, 149 (2000).
- [33] G. T. Horowitz and S. F. Ross, Phys. Rev. D **56**, 2180 (1997).
- [34] A. Lue and E. J. Weinberg, Phys. Rev. D **61**, 124003 (2000).
- [35] J. P. S. Lemos, “Gravitational magnetic monopoles and Majumdar-Papapetrou stars”, in preparation (2004).
- [36] W. Israel, Nuovo Cim. B **44**, 1 (1966).